NASA DEVELOP National Program
Virginia – Langley

Summer 2021

Fairfax County Urban Development

Identifying Urban Heat Mitigation Strategies for Climate Adaptation Planning in Fairfax County, Virginia

DEVELOP Technical Report

Final Draft – August 10th, 2021

W. Pierce Holloway (Project Lead)
Rose Eichelmann
Patricia Murer
Ryan Newell
Caden O'Connell

Advisors:
Dr. Kenton Ross, (NASA Langley Research Center)
Lauren Childs-Gleason, (NASA Langley Research Center)

1. Abstract

Extreme high temperatures lead to population vulnerabilities such as increased instances of heat-related illnesses, cardiovascular disease, pulmonary disease, and even death, as well as increased energy consumption and infrastructure costs. People in urbanized areas experience higher temperatures than rural areas due to diminished vegetation and increased impervious surfaces which absorb and radiate heat. Fairfax County, Virginia has embarked on Resilient Fairfax, a program aimed at addressing climate adaptation and resilience. The NASA DEVELOP team partnered with the Fairfax County Office of Environmental and Energy Coordination (OEEC) to assess the extent of the urban heat island effect in the county and its most vulnerable populations. The team used data from Landsat 8 Operational Land Imager (OLI) and Thermal Infrared Sensor (TIRS), as well as the ECOsystem Spaceborne Thermal Radiometer Experiment on Space Station (ECOSTRESS) for the years 2013 to 2021. The study found that the hottest spots were in densely urbanized areas, with land surface temperatures as much as 47°F above that of undeveloped reference area land surface temperatures. The team used the Integrated Valuation of Ecosystem Services and Tradeoffs (InVEST) urban cooling model and determined that areas with higher tree canopy cover had greater heat mitigation capacity. Estimates from the InVEST model showed that a 4.5% increase in canopy cover across the county could result in a temperature reduction of up to 2.4°F in some areas. The results will allow partners to assess heat distribution across Fairfax County and more effectively target and prioritize effective heat mitigation strategies.

Key Terms

urban heat island effect, land surface temperature, vulnerability, Landsat 8 TIRS, ECOSTRESS, InVEST, urban development, climate adaptation

2. Introduction

2.1 Background Information

Extreme temperatures threaten public health and infrastructure, especially in urban areas, which are home to over half of the world's current population (Li, 2013). Heatwaves have a severe impact on more developed areas because their land cover is comprised of less vegetation and more impervious surfaces. Tree canopies provide shade which has a cooling effect, as does the process of evapotranspiration by plants. In contrast, surfaces such as asphalt and concrete absorb more heat during the day and radiate that heat back into the atmosphere, causing urban areas to be warmer than nearby rural areas. This phenomenon is known as the urban heat island effect (UHI) (Arnell, 2019). National, state, and local governments are responding to increasing heat by developing heat mitigation plans that aim to protect their citizens, businesses, and infrastructure. Determining areas of high heat exposure and vulnerability are necessary to prioritize areas for mitigation efforts and effectively address the UHI effect. The threat of extreme heat is causing many urbanized districts including Fairfax County, VA to commission further research on urban heat and potential mitigation techniques.

Heatwaves in the United States are the deadliest type of weather event, with an average of 131 direct heat fatalities a year in the past 20 years (National Weather Service, n.d.). The CDC attributes 7,415 deaths in the United States to exposure of natural heat as the underlying or contributing cause of death from 1999 to 2010, an average of 618 per year (CDC, 2012). Extreme heat can result in various physiological reactions ranging from discomfort and dehydration to more serious conditions such as heat exhaustion and heatstroke (Epstein et. al, 2014). Other consequences include losses in labor productivity, increased energy consumption, and decreased learning (Hsu et. al, 2021). Certain populations are more sensitive to heat stress, such as children and the elderly, as well as people with pre-existing cardiovascular or respiratory illnesses (Rosenthal et.al, 2014). Furthermore, recent studies indicate the effects of urban heat have disproportionate impacts among marginalized and low-income communities (Hsu et. al 2021). Understanding the disproportionate impacts of the UHI effect on a community is crucial to identifying priority areas for cooling initiatives and mitigation strategies.

Fairfax County, VA, covers 406 square miles (1,010 km²) in the northern Virginia greater Washington, DC metropolitan region. The county surrounds Fairfax City, which is a separate jurisdiction. The county borders the Potomac River in the Southeast, as seen below in *Figure 1*. With about 1.12 million individuals and a median household income of $128,374, it is the most populated and among the most affluent counties in the state (Han and Khaja, 2021).

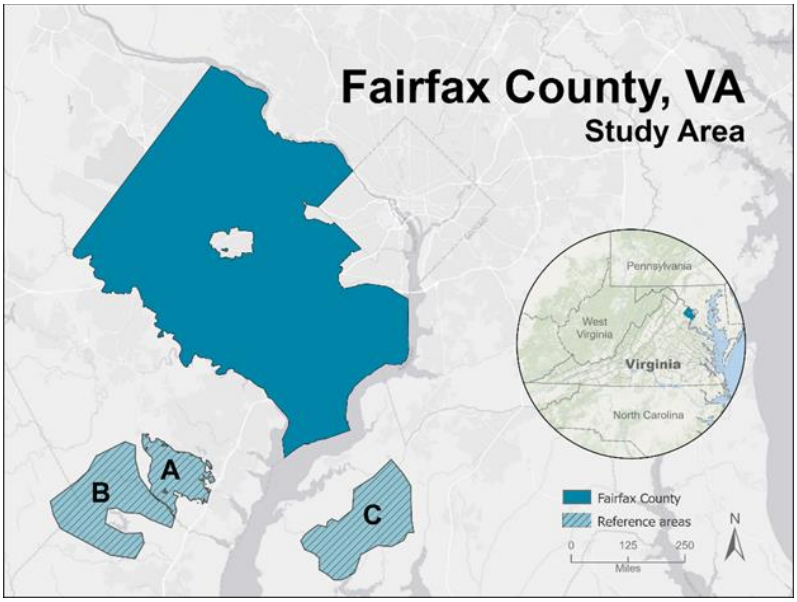

Figure 1. Study Area of Fairfax County, Virginia and reference areas:
(A) Prince William Forest Park and (B) Marine Corps Base Quantico in Prince William County, VA.,
(C) Glatfelter Easement and adjacent areas in St. Charles County, MD.
(County boundary source: https://www.fairfaxcounty.gov/maps/, ESRI Light Canvas base map)

The InVEST urban cooling model has been employed in previous research studies to model the impacts of urban development practices on UHI, target hotspots for mitigation, and to measure the cooling effects of heat-mitigation efforts (Kadaverugu et al. 2020). Bosch et al. used InVEST to show the correlation between land use and heat wave intensity in a Swiss urban environment (2021). Their study found that the InVEST tool outperformed previous climate assessment methods by incorporating the physical characteristics of the land and atmosphere, resulting in more accurate and dynamic predictive models.

2.2 Project Partners

This team partnered with the Fairfax County Office of Environmental and Energy Coordination (OEEC) on this project. The OEEC is interested in investigating UHI effects within the county, identifying the hottest spots, most vulnerable populations, and determining effective cooling strategies and priority areas for heat mitigation. Motivation to investigate UHI has also been underscored by public support for understanding how populations within the county may be disproportionately vulnerable to urban heat. Informed by the InVEST urban cooling model output, the OEEC will determine how factors such as increased tree canopy cover and albedo can be leveraged to improve the heat mitigation capacity of an area. The strategies informed by this study will be incorporated into the Resilient Fairfax: Climate Adaptation and Resilience Plan, to be completed in 2022.

3. Methodology

3.1 Data Acquisition

The team retrieved Landsat 8 TIRS Provisional Surface Temperature and OLI Surface Reflectance products included in the U.S. Landsat Analysis Ready Data (ARD) bundle for Fairfax County and surrounding areas for the months of June through August of 2013 to 2020 from the US Geological Survey Earth Explorer

website. The ECOsystem Spaceborne Thermal Radiometer Experiment on Space Station (ECOSTRESS) data from the USGS Application for Extracting and Exploring Analysis Ready Samples (AppEEARS) and NASA EarthData portals provided the nighttime land surface temperature (LST) and evapotranspiration data, respectively, for the months of June through August of 2018 to 2021(Hook 2019). *Table 1* contains the list of satellite platforms and sensors that produced the data.

Table 1.
NASA Earth Observations used in this study.

Platform	Sensor	Parameter	Date Range	Resolution
Landsat 8	Operational Land Imager (OLI)	Albedo	2013 - 2020 (June through August)	30 m
Landsat 8	Thermal Infrared Sensor (TIRS)	Daytime Land Surface Temperature (LST)	2013 - 2020 (June through August)	100 m
International Space Station (ISS)	ECOsystem Spaceborne Thermal Radiometer Experiment (ECOSTRESS)	Evapotranspiration Nighttime LST	2018 – 2021 (June through August)	70 m

The OEEC provided the county land use land cover (LULC) data as well as the canopy cover and building footprints shapefiles, all necessary inputs for the InVEST model. The team used the 2016 National Land Cover Database (NLCD) for the adjacent areas inside and around the county. The project partners also provided the socio-economic-health data based on the American Community Survey (ACS) 2014 - 2018 for the heat vulnerability analysis.

3.2 Data Processing for LST Imagery

3.2.1 Daytime LST

The team first removed any pixels from the daytime LST data that were tainted by the presence of clouds or cloud shadows. The Landsat Collection 1 Level-1 Quality Assessment band contains information on the usability of pixels within a Landsat scene, allowing users to apply filters on pixels containing clouds, water, or snow. The team developed a Python script which utilized the Quality Assessment raster provided within each LST product to mask pixels values classified as cloud, high-confidence cloud, medium-confidence cloud, high-confidence cirrus, and cloud-shadow. The team then used the Cell Statistics tool in QGIS to calculate a mean value for each pixel across the 82 cloud-masked daytime LST images, outputting a mean daytime LST raster that the team used to derive the daytime LST anomalies.

The Landsat 8 Provisional Surface Temperature Product is in units of degrees Kelvin with a scale factor of 0.1, so the team used Eq. (1) in QGIS along with the Raster Calculator tool to convert the units into degrees Fahrenheit.

$$\boldsymbol{Fahrenheit\,(°F) = Kelvin * 0.1 * 1.8 - 459.67} \qquad \text{Eq. (1)}$$

3.2.2 Nighttime LST

The team filtered the downloaded ECO2LSTEv001 dataset and filtered the images for nighttime hours and the hot months using R code built in RStudio to process only the images acquired for times between 9:00 p.m. and 5:00 a.m. local time, between June 1st and August 31st each year of the study period. The team then used the quality bands in the ECO2LSTEv001 dataset to identify clouded or low-quality pixels in the LST dataset and to remove the data from those pixels, such that measurements of cloud temperature do not contaminate the calculations for mean LST. Specifically, the team applied a filter to omit LST pixels flagged with "cloud detected" or "bad/missing data" in the quality control band. Following masking and filtering, the team used the r.series tool in QGIS to calculate mean values for each pixel from the 29 resulting images to produce a raster layer of mean nighttime LST. The team used shapefiles for Fairfax County and the reference

areas to clip that mean nighttime LST layer and produce mean nighttime LST values for the study area and reference areas. The team converted the acquired values to Kelvin by multiplying each by a factor of 0.02.

3.3 Data Processing for Daytime and Nighttime LST Anomalies

To evaluate the UHI effect, the team needed to compare the county temperatures to those of undeveloped forested areas. The team selected Prince William Forest Park and the Marine Corps Base Quantico in Prince William County, VA., and the Glatfelter Easement and adjacent areas in St. Charles County, MD, as reference areas, based on these criteria: altitude and latitude similarity, positioned away from major water bodies, and within 50 miles of the county (*Figure 1*).

The team processed LST of the reference areas according to the process outlined in the earlier sections, and further calculated the mean reference temperatures by finding the average daytime and nighttime temperatures across the study period for the reference areas. The team derived the temperature anomaly by subtracting the mean reference temperature from each pixel of the daytime and nighttime LST products. In addition to calculating the LST anomaly using the reference areas, the team mapped the heat anomalies as a difference from the Fairfax County mean temperature. In this exercise, the team calculated a single mean value from the Fairfax County daytime LST raster and subtracted that value from each pixel within the daytime LST map. The resulting map shows the average temperature difference between a given pixel and the spatial mean daytime temperature of Fairfax County.

In nighttime LST anomaly map generation, the team aimed to reduce unnecessary influence of day-to-day temperature variation on the final anomaly products by removing the daily county mean from each individual scene. The team clipped each scene to the county and reference area shapefiles immediately following masking, prior to generating average maps. The team calculated the mean LST value for each clipped scene and subtracted it from each pixel, resulting in anomaly maps for each acquisition day. The team averaged each of those daily anomaly maps to generate mean nighttime LST anomaly maps for the county and reference areas. The resulting map, generated from data clipped to the county, represented the nighttime LST anomaly with respect to the county, and to generate nighttime LST anomaly with respect to the reference areas, the team calculated mean values from the county and reference areas using the overall mean LST map (described in the preceding paragraph) and subtracted the difference from the county LST anomaly map.

3.4 Heat Vulnerability Analysis

The team created a heat exposure index and a heat sensitivity index for each census tract and used these to produce a heat vulnerability index to display the most heat vulnerable regions throughout the county. To calculate heat exposure, the team used Eq. 2, where mDLST is mean daytime LST and mNLST is mean nighttime LST. Literature suggests that nighttime temperatures are better predictors of heat-related health consequences (Murage et al., 2017) and consequently the nighttime LST has a greater influence on the exposure index. Following calculation of an exposure raster, the team used zonal statistics to calculate mean exposure for each census tract, then reclassified those exposures to index values between one and five using natural breaks.

$$\boldsymbol{Exposure} = \frac{\boldsymbol{mDLST} * \mathbf{0.5} + \boldsymbol{mNLST}}{\mathbf{1.5}} \qquad \text{Eq. (2)}$$

The project partners provided the team with 15 socio-economic datasets they believed were pertinent for identifying heat-sensitive populations. They already had ranked each individual variable into 5 classes using natural breaks and given a score 1 - 5, with 5 being the most sensitive. The team collected 3 additional datasets from the ACS and conducted the same scoring methodology as the county. The team grouped the variables into four sub-indices: income, health, demographics, and housing, which can be seen in *Table A1*. Then, the team averaged the scores of all the variables within each sub-index to calculate an overall score per census tract for that sub-index. To get an overall sensitivity score for each census tract, the team averaged all the sub-indices and used natural breaks to rank the scores 1 - 5.

The team created the heat vulnerability index by compounding the heat exposure index score with the heat sensitivity index score, derived by Eq. (3).

$$\textbf{\textit{Heat Vulnerability} = \textit{Heat Exposure} * \textit{Heat Sensitivity}} \quad \text{Eq. (3)}$$

As an alternate methodology, the team attempted to calculate the vulnerability index by conducting a Principal Component Analysis (PCA) of the heat sensitivity variables. PCA is a statistical procedure which reduces the dimensionality of a dataset while retaining as much of the variance within the dataset as possible, achieved through the creation of a new set of uncorrelated variables, the principal components. However, the team had to throw out the first principal component due to its contradicting correlations, greatly reducing the variance explained by the chosen components. For this reason, the team decided not to pursue this methodology for the vulnerability analysis.

3.5 Data Processing for the InVEST Model

3.5.1 Land Use Land Cover (LULC)

The InVEST model considers the influence of large green areas up to a 2 km distance when calculating heat mitigation capacity. Since the Fairfax County LULC GIS data did not include data for its roads, Fairfax City, or areas bordering the county, the team adapted the 2016 National Land Cover Database (NLCD) to fill in the missing information. The NLCD classifications differed from the categories used by Fairfax County and based on judgment, the team reclassified the NLCD classifications to match the Fairfax County-provided layer. Lastly, they added two land use categories of high and low intensity road.

The team used the combined raster as the foundation for the biophysical table required by InVEST, where they assigned values for shade, albedo, crop coefficient, and building intensity for each unique LULC classification. See *Figure 2* below for the Fairfax County LULC categories map utilized by this study.

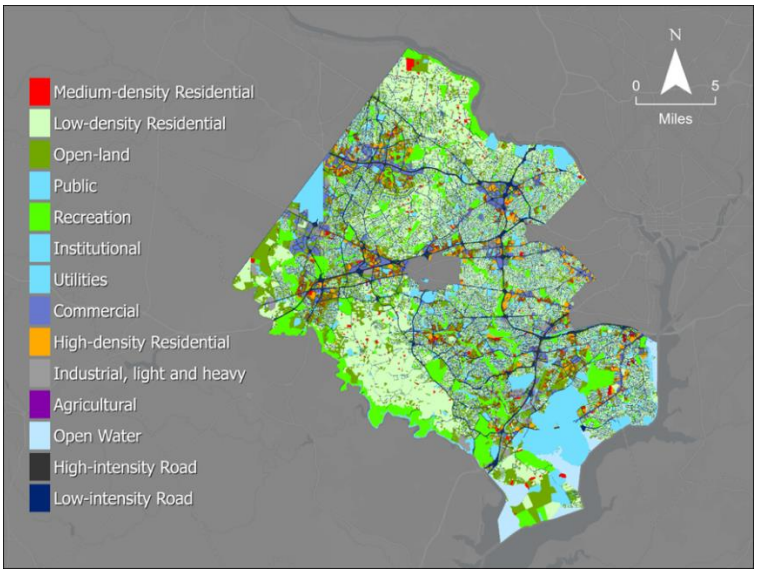

Figure 1. Fairfax County Land Use Land Cover categories adapted for the study.

3.5.2 Building Intensity

Accounting for built infrastructure is crucial to understanding nighttime temperatures as structures absorb solar radiation throughout the day and release this stored energy in the evening. The building footprint vector file covering both Fairfax County and city contained building footprint area (Ba) and respective relative height. To determine the average ceiling height for each building, the team used an approximation of 7.5 feet in residential buildings and 10 feet in commercial buildings as described in Chun and Guldmann (2021). The

team divided relative building height by its respective building ceiling height approximation to estimate the numbers of floors in the building (F), rounding to the nearest whole number and replacing zeros with a value of one. The team then multiplied the number of floors by the building footprint to determine total building floor area. The team calculated building intensity for each LULC for the biophysical table as a normalized value between 0 and 1 by dividing the total building floor area across all buildings in each LULC by the cumulative area of the corresponding LULC, according to Eq. (4).

$$BI\ (unitless) = \Sigma(B_a \times F) \div L_a \quad \text{Eq. (4)}$$

where BI is the building intensity for each LULC class, B_a is the building footprint for each LULC class (m^2), F is number of floors, and L_a is the land area for each LULC class (m^2). The team then spatially joined building intensity results to respective LULC pixel to provide a set of values for use in the biophysical table.

3.5.3 Shade

The team calculated shade starting with a vector shapefile depicting canopy coverage in a binary form (tree/no tree), which was converted into a raster and clipped to the study area. The canopy cover across Fairfax County is shown in *Figure B1*. Then, the team created a fishnet grid (with each grid square ~30 m x 30 m) encompassing the study area, serving as a zone field to compute percent canopy coverage for each grid square. The team combined this new gridded area containing county's percent canopy cover to the National Land Use Cover 2016 US Forest Service Tree Canopy Cover using the union tool to create a seamless layer for the study area, encompassing both the county and reference areas. Canopy coverage was then calculated for each land use area using a 2 km buffer around the county to deliver a more accurate representation of canopy coverage at the county boundaries.

3.5.4 Albedo

Albedo represents the proportion of solar radiation reflected by a surface. High albedos closer to 1 are typical for snow and deserts, which reflect large fractions of the sunlight while albedos close to zero are typical of oceans and lakes. Low albedos for vegetation indicate that the surfaces absorb most of the incoming energy, temporarily "sinking" the heat and improving cooling capacity (Coakley, 2003). Consequently, the InVEST model includes the average albedo for each land use category in its calculations of heat mitigation capacity. The team calculated the mean albedo from the surface reflectance data of the blue, green, red, near infrared (NIR), short-wave infrared (SWIR1 and SWIR2) bands with the "Olmedo weighted coefficients" (Olmedo et.al, 2016) using Eq. (5). The resulting map of albedo across Fairfax County is shown in *Figure B2*.

$$Albedo = Blue * 0.246 + Green * 0.146 + Red * 0.191 + NIR * 0.304 + SWIR1 * 0.105 + SIR2 * 0.008 \quad \text{Eq. (5)}$$

3.5.5 Evapotranspiration (ET)

ECOSTRESS Evapotranspiration (ET) data included a quality assessment (QA) product, assigning raster pixels values based on their cloud cover levels. This data set included layers titled ETDaily, measuring the daily latent heat flux of Fairfax County over our study period. The team used a model within ArcGIS Pro to convert the units of this layer into the format required by the InVEST model [mm day^{-1}] using Eq. (6):

$$ET_A\ [mm\ day^{-1}] = ET_B\ [W\ m^{-2}] * 0.0864 \frac{[MJ\ day^{-1}]}{[W]} * 0.408 \frac{[mm\ day^{-1}]}{[MJ\ day^{-1} m^{-2}]} \quad \text{Eq. (6)}$$

ET_A is the unit-converted numerical rate of ET used in the InVEST model [mm day^{-1}] and ET_B is the ET value before conversion [$W \cdot m^{-2}$]. The team used a Python script to remove all clouded pixels from the ET raster by using the QA flags and then averaged all of the images using the Cell Statistics tool. This produced the median ET image needed to run the InVEST model, as shown in *Figure B3*. Due to irregularities present within the ETDaily minimum values, the team used the median rather than mean to represent the data and reduce the effect of outliers. Since ECOSTRESS does not provide ET data over water, the team filled those

pixels with the median ET value of the image (74,131), using the 'is null' tool in ArcGIS Pro to find pixels with no data value and the 'con' tool to set a new value.

3.5.6 Crop Coefficient (K_c)

The crop coefficient is used by the InVEST model to determine the actual evapotranspiration from the potential evapotranspiration. The ECOSTRESS evapotranspiration data utilized by the team is already estimated as actual evapotranspiration, and as such, the crop coefficient is not necessary. For this reason, the team used a constant K_c value of 1 for each LULC class within the biophysical table, as to not interfere with the actual evapotranspiration values derived from ECOSTRESS.

3.5.7 *Mitigation Scenario*

The team developed a mitigation scenario of altering the canopy cover amounts in the biophysical table to estimate impacts of potential shade increase across the county. The amount of canopy cover increase was chosen arbitrarily and does not represent the team's opinions of possible policy interventions in Fairfax County. The impetus behind this exercise was to test the InVEST model's capability to project hypothetical changes and their impacts on heat mitigation. The following land use cover categories were increased: Industrial light-heavy (20%); High-density residential, Medium-density residential, Commercial (15%); Public & Utilities (10%); Low-intensity-road (8%); Agricultural & Low-density residential (5%).

4. Results & Discussion

4.1 Analysis of Results

4.1.1 Heat Anomalies

Using LST data from Landsat 8 and ECOSTRESS, the team produced daytime and nighttime heat anomaly maps. The team calculated temperature anomalies with respect to both the county mean LST and the reference area mean LST. The various heat anomaly maps are shown in *Figure 3*. *Figures 3a* and *3b* show the daytime anomalies in relation to the reference area and county means respectively, while *Figures 3c* and *3d* show the same relationships for nighttime anomalies. Temperature anomalies of 37°F (daytime) and 10°F (nighttime) over the county mean were observed, meanwhile in respect to the reference area mean, there were temperature anomalies of 47°F (daytime) and 14°F (nighttime).

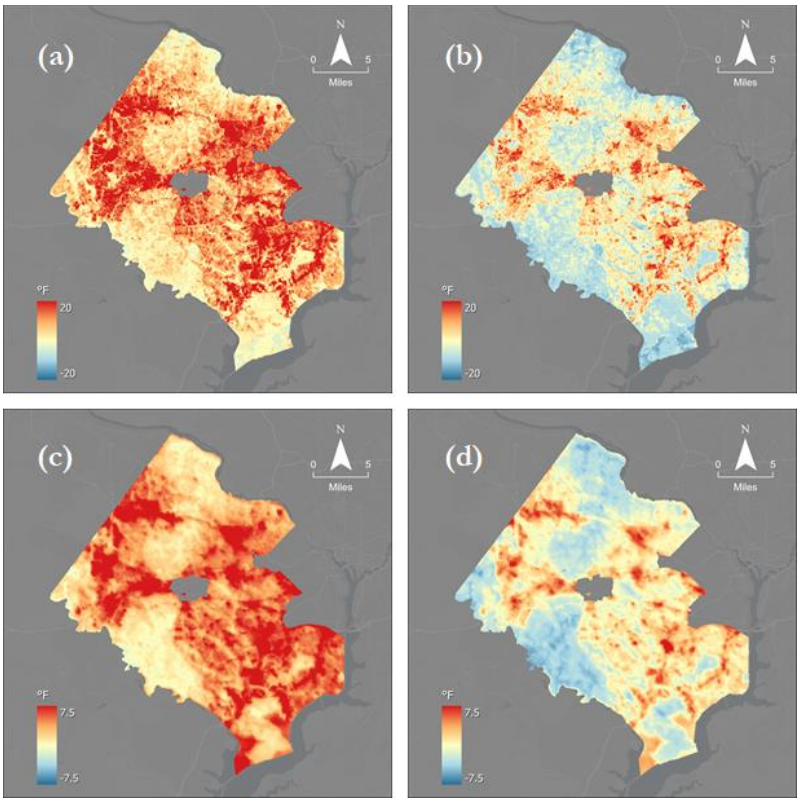

Figure 3. Fairfax County heat anomaly maps, showing daytime anomalies in relation to reference *(a)* and county *(b)* means, and nighttime anomalies in relation to reference *(c)* and county *(d)* means.

With consideration toward the physiology of Fairfax County, the team evaluated correlation of daytime LST with two variables: canopy cover and impervious surface cover. The daytime mean LST temperature of Fairfax County is shown in *Figure 4*. The team calculated mean daytime LST, canopy cover, and impervious surface cover by census block group and evaluated the correlations. *Figure 4a* shows the relationships between canopy cover and mean daytime LST and *Figure 4b.* shows the relationships between impervious surface cover and mean daytime LST. The values for daytime mean LST, canopy cover, and impervious surface cover are recorded by block group GEOID in the supplementary data documentation.

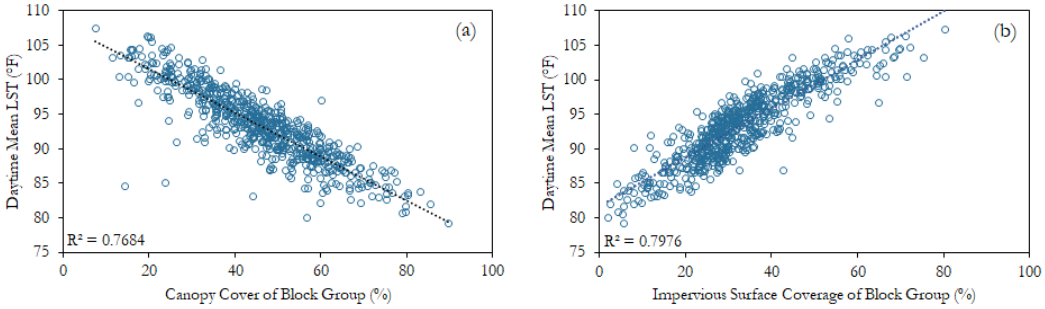

Figure 4. Plots showing correlation between block group canopy cover and daytime mean LST (°F) (a), and correlation between block group impervious surface coverage and daytime mean LST (°F) (b)

The evident relationship prompted significance testing, and the Pearson correlation coefficients demonstrated a strong relationship in each of the two variable pairs, with values of -0.877 for canopy cover and LST, and 0.893 for impervious surface cover and LST. The results suggest a strong and approximately linear relationship in both pairs over the range studied, with the correlation being negative between canopy cover

and LST, and positive between impervious surface cover and LST. The patterns indicate that areas with high impervious surface cover and low canopy cover are expected to have the highest mean LST. Inspection of the daytime heat anomaly maps reveals that the most urbanized areas, characterized by extensive impervious surfaces and relatively low tree cover, did exhibit some of the highest mean observed temperatures in this study.

4.1.2 InVEST HMI and Air Temperature

The team used the InVEST urban cooling model to generate an approximate output of the Heat Mitigation Index (HMI) for Fairfax County. HMI is a unitless value approximation of an areas ability to mitigate heat or cool itself. The InVEST model considers values of shade, evapotranspiration, albedo, and distance from cooling islands (e.g., parks) to generate its values ranging from 0 (no ability to mitigate heat) to 1 (ability to cool completely). The team ran two models to account for the daytime HMI as well as the nighttime HMI. The nighttime conditions are calculated slightly different from the daytime as it considers building intensity within each land classification as its main determinate factor.

The team found that based on current conditions within the area the average daytime HMI for Fairfax was 0.42. *Figure 5a* shows the distribution of HMI values across the county. Additionally, the team found that the average nighttime HMI was 0.82. *Figure 5b* below illustrates the nighttime HMI values across the study area. More detailed analysis revealed that more urbanized areas had lower HMI values. The land classes with the two lowest HMI values were Commercial and High-Intensity Road, 0.244 and 0.273 respectively. Contrastingly the land classes with the two highest were Recreation and Open land, not forested or developed with average HMI values of 0.542 and 0.506 respectively.

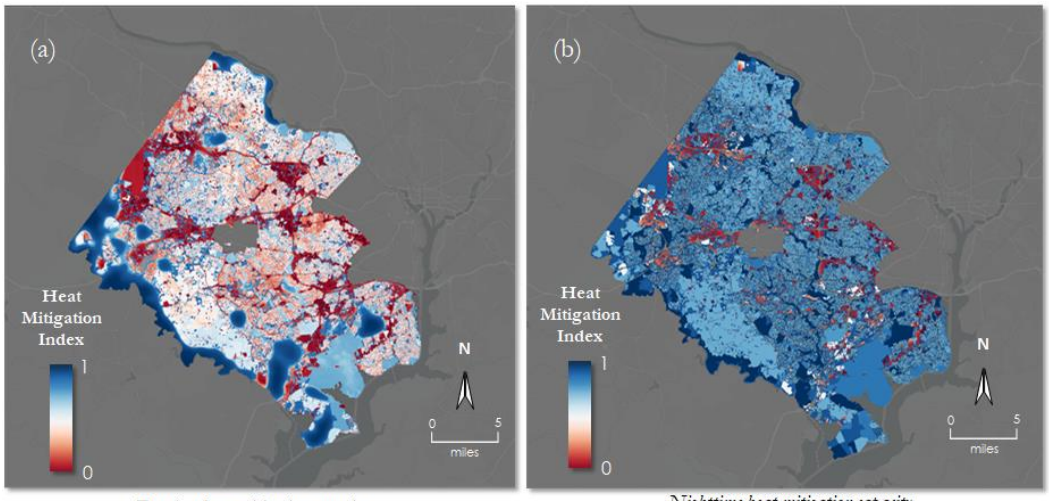

Figure 5. Fairfax County daytime HMI *(a)* and nighttime HMI *(b)* on a scale from 0 (red) to 1 (blue).

Along with the ability to model a HMI index for the county, the InVEST model generated maps of county air temperature. It was found that the county average daytime air temperature was 106.7 °F and the county average nighttime air temperature was 78.6°F. Further analysis showed that the land classes with the two highest average daytime temperatures were Commercial and High-density Residential, 109.2°F and 108.8°F each. While the two land cover classes with the lowest average daytime temperatures were Open land, not forested or developed and Recreation, having values of 105.7°F and 103.8°F respectively. Commercial areas stayed consistently hot in the nighttime, having the highest average nighttime temperature at 79.9°F. While Open Water had the lowest average nighttime temperature of 77.1°F.

4.1.3 InVEST Mitigation

The InVEST Urban Cooling model offers a powerful opportunity to alter conditions in the biophysical table to project the impacts of hypothetical changes to canopy cover, albedo, or building intensity. The team determined that a mitigation scenario of increasing canopy cover would be the most impactful variable to alter. This was due to preliminary analysis showing little impact from Albedo change in addition to past projects finding albedo alternations resulting in little to no change (LaJoie et al. 2021).

The team ran the InVEST model for daytime conditions altering only canopy cover and keeping all other factors consistent with the baseline. They found that a collective 4.5% increase in canopy cover across the county could result in a temperature reduction of up to 2.4°F in some areas. More detailed analysis revealed that the public land cover class experienced the largest area temperature reduction of 1.6°F.

4.1.4 Vulnerability

Results from the heat vulnerability analysis aid in determining which regions within Fairfax County are both more sensitive and have higher exposure to heat than other regions. The Heat Exposure Index, displayed in Figure 6a, illustrates similar patterns to the heat anomaly maps, with more urbanized census tracts exhibiting hotter temperatures. Areas most impacted by high heat exposure included Tyson's Corner, Merrifield, Centreville, Springfield, Reston, Huntington, and Fair Lakes. Census tract 51059491303 had the highest heat exposure with a weighted mean temperature of 86.3 °F (*Table A2*). Areas with the lowest heat exposure scores included regions in South Central and North Central Fairfax County.

The Heat Sensitivity Index (*Figure 6b*) shows a somewhat different pattern than that of the Heat Exposure Index; some areas that had high exposure scores had low sensitivity scores and vice versa. However, some of the hottest areas did coincide with the most sensitive areas, such as Springfield. Some of the other most heat sensitive neighborhoods included Annandale, Hybla Valley, Seven Corner's and Bailey's Crossroads. A list of the top 10 heat sensitive tracts can be found in *Table A3*, with census tract 51059451400 scoring as the most heat sensitive. Some of the less sensitive areas include Oak Hill and Western-most Fairfax County.

The Heat Vulnerability Index (*Figure 6c*), as a result of heat sensitivity and heat exposure, illustrates the distribution of vulnerable regions within the county. The highest heat vulnerability scores were found in the areas of Springfield, Seven Corner's, Bailey's Crossroads, and Huntington. *Table A4* displays the top 10 most vulnerable census tracts.

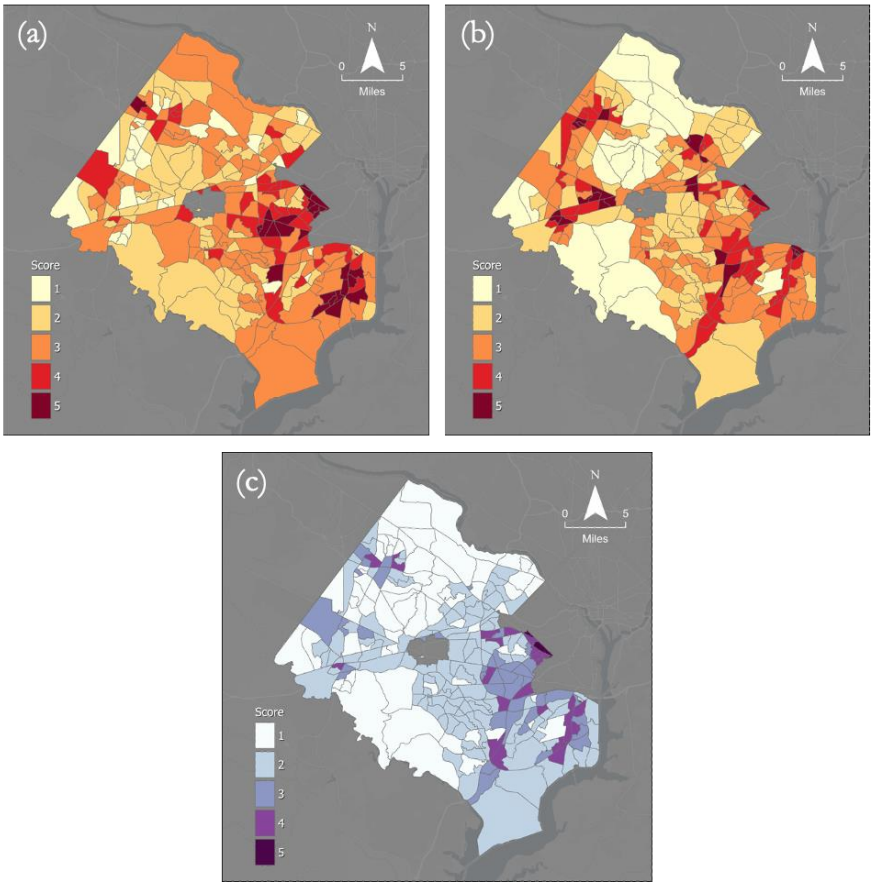

Figure 6. Heat Exposure Index with score of 5 being most exposed (a), Heat Sensitivity Index with score of 5 being most sensitive (b), and Heat Vulnerability Index with score of 5 being most vulnerable (c). The team divided the actual Heat Vulnerability Index values by 5 (Table A4) so the scale would align with other indices for visualization purposes.

As previously mentioned, the team decided not to conduct the heat vulnerability analysis using results from the PCA. This was because the first principal component, which retained 33% of the variance within the dataset, was thrown out. Variables that weighed heavily upon this component included old age with a positive loading factor, and poverty, with a negative loading factor. In other words, within Fairfax County, an increase in age is associated with a decrease in poverty. This complicated interpretation of the results because old age is associated with higher heat sensitivity while more wealth is associated with lower heat sensitivity. The team was unsure whether higher values in component one should be associated with high or low sensitivity risk, thus the reasoning for throwing out the first component and retaining components two through five instead. However, in doing so the variance of the dataset was greatly reduced, and the team decided this methodology would not produce an accurate depiction of heat vulnerability within the county.

4.2 Future Work

Future work could refine the heat vulnerability index by further analyzing the public's daily routine, which could increase the accuracy of the heat sensitivity index and discern the effect of daytime or nighttime heat in relation to the most frequented locations throughout the day. One limitation of the vulnerability analysis was that the grouping of variables into larger sub-indices was subjective and somewhat arbitrary. Future work could compare results from our heat vulnerability index obtained from subjectively grouping the component variables with an index produced using PCA. Research could also be conducted to determine whether some variables should be weighted more than others when it comes to determining heat vulnerability. In addition,

the city's development patterns, and zoning practices could be analyzed to determine the influence of past planning decisions on of the presence of current UHI.

In order to improve the results of the InVEST model, future work could refine input datasets. Certain rasters of the input datasets had 'NoData' pixels that the team had to estimate for. The team needed to revise some InVEST results as well to preserve the accuracy of the product. Possible future work includes collecting additional datasets to calculate the true rate of evapotranspiration over water bodies and reassessing the representation of roads in InVEST input layers. The InVEST Model flagged roads as areas with very high cooling capacity when in reality they retain heat during the day and slowly release it at night. Therefore, the team had to remove all InVEST outputs on roads to correct this. Future work could also include the collection of additional data to generate an Energy Savings Table, allowing for the financial impact of UHI as well as potential savings due to heat mitigation to be an end product.

Lastly, future work could reassess the study's methodology and improve the accuracy of the overall results by using an algorithm that references the ECOSTRESS tiles properly before processing. These tiles have slight geo-positional variances that reduced the accuracy of the data when averaging multiple images. Also, surface temperature results from the provisional data set could be compared with results obtained from downloading and processing the data with a Google Earth Engine script.

5. Conclusions

Some areas within Fairfax County experienced day and nighttime temperatures similar to the temperatures of rural reference areas. However, like many urban jurisdictions, our study found the county had urban heat islands with high heat anomalies and temperatures upwards of 40°F above that of the reference areas and the county. These hotspots corresponded to areas of high building intensity in commercial, business, industrial, and residential zones as well as along highways.

Heat sensitive populations are more vulnerable when working and living in areas of high heat exposure during the day and returning home to an area of high nighttime temperature in the evening. The combination of sustained high temperatures during the day and not being able to cool off at night is dangerous to human health. Sustained heat stress does not allow the body to rest and exacerbates medical conditions. Therefore, addressing the effects of UHI on public health requires heat mitigation initiatives to focus on residential areas, and not solely regions with the highest heat exposure.

The HMI results from the InVEST model followed a similar pattern of spatial distribution as the heat anomalies. Areas in the county with a high density of impervious surfaces absorb more heat and have less tree canopy, resulting in a low heat mitigation capacity. Additionally, urbanized areas next to parks and forested land experience lower temperatures and a higher heat mitigation capacity.

The InVEST model also suggested that efforts to increase albedo have relatively little effect in reducing temperatures around the county. Other studies have noticed similar results. According to the InVEST model, increasing tree canopy is a more effective heat mitigation strategy. If Fairfax County increased tree canopy by 4.5%, the temperature could be reduced by 2.4°F in some areas.

It is a goal of the Fairfax County OEEC to use these results to evaluate the effectiveness of the cooling center locations. The heat vulnerability map with cooling center locations overlayed indicated that not all areas of high heat vulnerability are within one mile of a cooling center. However, the areas not within one mile may not be highly populated. Therefore, further analysis is needed to assess the effectiveness of current cooling center locations.

The OEEC will be able to utilize the results of this study within their Resilient Fairfax: Climate Adaptation and Resilience Plan. The vulnerability analysis will help inform partners of areas within Fairfax County that should be prioritized for mitigation efforts, allowing the county to visualize the distribution of populations

that are most sensitive, exposed, and vulnerable to heat. Results from the InVEST model will help partners understand the effects of different land cover types on heat mitigation capacity and the cooling potential of planting more trees across the county.

6. Acknowledgments

A special thank you to Dr. Kenton Ross (NASA Langley Research Center), Lauren Childs-Gleason (NASA Langley Research Center), Dr. David Hondula (Associate Professor for the School of Geographical Science and Urban Planning at Arizona State University), and Adriana LeCompte (Fellow DEVELOP Langley node) for their science advice, guidance, feedback, and support through the project, and to our partners Allison Homer, Matthew Meyers, and Stephanie Cornejo from the Fairfax County Office of Environmental and Energy Coordination for generously sharing the history of Fairfax County urbanization and regulatory framework, forestry initiatives, and their feedback on our work.

Any opinions, findings, and conclusions or recommendations expressed in this material are those of the author(s) and do not necessarily reflect the views of the National Aeronautics and Space Administration.

This material is based upon work supported by NASA through contract NNL16AA05C.

7. Glossary

Albedo - the fraction of light reflected by a surface

Earth observations – Satellites and sensors that collect information about the Earth's physical, chemical, and biological systems over space and time

ECOsystem Spaceborne Thermal Radiometer Experiment on Space Station (ECOSTRESS) - satellite mission that aims to measure how the terrestrial biosphere changes in response to environmental changes such as water availability.

Evapotranspiration – the sum of evaporation of water from land and other surfaces and through transpiration by plants

Heat Anomaly - temperatures higher than a reference temperature

Heat Exposure – the magnitude of heat energy in a given area

Heat Mitigation Index (HMI) - value approximation of an areas ability to mitigate heat or cool itself

Heat Sensitivity Index – aggregate score of health, economic, social and demographic variables that make an individual experience more severe consequences if exposed to heat.

Heat Vulnerability Index – numerical score from the product of heat sensitivity and heat exposure

Integrated Valuation of Ecosystem Services and Tradeoffs (InVEST) - a suite of models used to map and value the goods and services from nature that benefit human life

Land Surface Temperature (LST) - temperature of the surface of the Earth

Operational Land Imager (OLI) - sensor aboard the Landsat 8 satellite that measure visible, near infrared and shortwave infrared wavelengths

Thermal Infrared Sensor (TIRS) - sensor aboard the Landsat 8 satellite that measures both Earth's surface temperature and atmospheric temperature

Urban Heat Island (UHI) Effect – difference in temperature between and urban area and an undeveloped or more natural forested area

8. References

Arnell, N. W., Lowe, J. A., Challinor, A. J., & Osborn, T. J. (2019). Global and regional impacts of climate change at different levels of global temperature increase. *Climatic Change*, *155*(3), 377–391. https://doi.org/10.1007/s10584-019-02464-z

Bosch, M., Locatelli, M., Hamel, P., Remme, R. P., Chenal, J., & Joost, S. (2021). A spatially explicit approach to simulate urban heat mitigation with InVEST (v3.8.0). *Geoscientific Model Development*, *14*(6), 3521–3537. https://doi.org/10.5194/gmd-14-3521-2021

Centers for Desease Control and Prevention. (2012) *QuickStats: Number of Heat-Related Deaths, * by Sex — National Vital Statistics System, United States,† 1999–2010§*. https://doi.org/10.1186/2046-7648-3-14

Chung, B., Guldmann, J.M. (2012). Two- and Three-Dimensional Urban Core Determinants of the Urban Heat Island: A Statistical Approach. *Journal of Environmental Science and Engineering* B, 1 (3), 363-378. https://www.researchgate.net/publication/261760149_Two-_and_Three-Dimensional_Urban_Core_Determinants_of_the_Urban_Heat_Island_A_Statistical_Approach [Last accessed Aug. 12, 2021]

Coakley, J.A. (2003). Reflectance and Albedo, Surface. *Encyclopedia of Atmospheric Sciences*, 1914-1923. https://doi.org/10.1016/B0-12-227090-8/00069-5

Han, X., & Khaja, F. (2021). Demographic Reports 2020. https://www.fairfaxcounty.gov/demographics/sites/demographics/files/assets/demographicreports/fullrpt.pdf.

ECOSTRESS L3/L4 Ancillary Data Quality Assurance (QA) Flags L3 Global 70 m V001 – ECO3ANCQA Hook, S., Fisher, J. (2019). ECOSTRESS L3/L4 Ancillary data Quality Assurance (QA) flags L3 Global 70 m V001 [Data set]. NASA EOSDIS Land Processes DAAC. doi: 10.5067/ECOSTRESS/ECO3ANCQA.001

Hook, S., Fisher, J. (2019). *ECOSTRESS Evapotranspiration PT-JPL Daily L3 Global 70 m V001*. NASA EOSDIS Land Processes DAAC. Accessed 2021-06-29 from https://doi.org/10.5067/ECOSTRESS/ECO3ETPTJPL.001. Accessed June 29, 2021.

Hook, S., Smyth, M., Logan, T., Johnson, W. (2019). *ECOSTRESS Geolocation Daily L1B Global 70 m V001*. NASA EOSDIS Land Processes DAAC. Accessed 2021-06-29 from https://doi.org/10.5067/ECOSTRESS/ECO1BGEO.001. Accessed June 29, 2021.

Hook, S., Hulley, G. (2019). *ECOSTRESS Land Surface Temperature and Emissivity Daily L2 Global 70 m V001* [Data set]. NASA EOSDIS Land Processes DAAC. doi: 10.5067/ECOSTRESS/ECO2LSTE.001

Hsu, A., Sheriff, G., Chakraborty, T., & Manya, D. (2021). Disproportionate exposure to urban heat island intensity across major US cities. *Nature Communications*, 12, 2721. https://doi.org/10.1038/s41467-021-22799-5

Kadaverugu, R., Gurav, C., Rai, A., Sharma, A., Matli, C., & Biniwale, R. (2021). Quantification of heat mitigation by urban green spaces using InVEST model—a scenario analysis of Nagpur City, India. *Arabian Journal of Geosciences*, *14*(2). https://doi.org/10.1007/s12517-020-06380-w

LaJoie, P. Cronin-Golomb, O. Feibel, S. Rokosz, K. (2021) Assessing Urban Heat in the Cincinnati and Covington Area using NASA Earth Observations [Unpublished scientific manuscript]. NASA DEVELOP.

Li, D., & Bou-Zeid, E. (2013). Synergistic Interactions between Urban Heat Islands and Heat Waves: The Impact in Cities Is Larger than the Sum of Its Parts. *Journal of Applied Meteorology and Climatology*, *52*(9), 2051–2064. https://doi.org/10.1175/jamc-d-13-02.1

Lucas, R. A., Epstein, Y., & Kjellstrom, T. (2014). Excessive occupational heat exposure: a significant ergonomic challenge and health risk for current and future workers. *Extreme physiology & medicine*, 3(1), 1-8. https://doi.org/10.1186/2046-7648-3-14

Murage, P., Hajat, S., & Kovats, R. S. (2017). Effect of night-time temperatures on cause and age-specific mortality in London. Environmental Epidemiology (Philadelphia, Pa.), 1(2), https://doi.org/10.1097/EE9.0000000000000005

National Weather Service. (n.d.). Weather Fatalities 2020. https://www.weather.gov/hazstat/

Olmedo, G. F., Ortega-Farias, S., de la Fuente-Saiz, D., Fonseca-Luego, D., Fuentes-Penailillo, F. (2016). Water: tools and function to estimate actual evapotranspiration using land surface energy balance models in R. *The R Journal*, 8:2, 352-369. https://doi.org/10.32614/RJ-2016-051

Rosenthal, J. K., Kinney, P. L., & Metzger, K. B. (2014). Intra-urban vulnerability to heat-related mortality in New York City, 1997–2006. *Health & Place,* 30, 45-60. https://doi.org/10.1016/j.healthplace.2014.07.014

9. Appendices

Appendix A: Additional inputs and findings from vulnerability study.

Table A1.
Overview of sensitivity index sub-indices and their associated American Community Survey (ACS) socio-economic variables.

Sensitivity Factor	ACS Datasets
Income	Below Poverty Line Median Household Income Severely Burdened Renter No vehicle
Health	Population without health insurance Population with a disability Adults with hypertension Adults with COPD Adults with asthma Adults with diabetes Adults reported as obese
Demographics	Age 65 & over Age 5 & under Population that speaks English "less than well"
Housing	Overcrowding Populations in nursing homes Populations incarcerated Mobile Homes

Table A2.
Heat Exposure Score table displaying top 10 scoring census tracts.

GEOID	Mean Temperature (°F)	Exposure Score
51059491303	86.3	5
51059420400	85.9	5
51059482203	85.6	5
51059491202	85.4	5
51059452802	85.4	5
51059440201	85.3	5
51059421002	85.1	5
51059420503	85.0	5
51059481101	85.0	5
51059480203	84.9	5

Table A3.
Heat Sensitivity Score table displaying top 10 highest scoring (most sensitive) tracts.

GEOID	Income Score	Demographic Score	Health Score	Housing Score	Sensitivity Score
51059451400	4.500	4.333	3.500	1.000	5
51059452802	4.500	3.000	4.333	1.333	5
51059451502	3.750	3.667	4.000	1.667	5
51059421500	4.000	3.000	3.667	2.333	5
51059421600	4.750	3.000	4.167	1.000	5
51059415500	4.000	3.000	4.167	1.667	5
51059451501	4.750	3.667	3.333	1.000	5
51059421701	4.250	3.333	4.000	1.000	5
51059421400	4.250	3.333	3.833	1.000	5

51059431600	4.250	3.000	3.500	1.667	5

Table A4.
Heat Vulnerability Score table displaying the top 10 scoring (most vulnerable) tracts.

GEOID	Exposure Score	Sensitivity Score	Vulnerability Score
51059451400	5	5	25
51059420501	5	5	25
51059451502	5	5	25
51059452802	5	5	25
51059415401	4	5	20
51059416000	4	5	20
51059421400	4	5	20
51059421500	4	5	20
51059421600	4	5	20
51059421701	4	5	20

Appendix B: Auxiliary Maps Used in Calculations

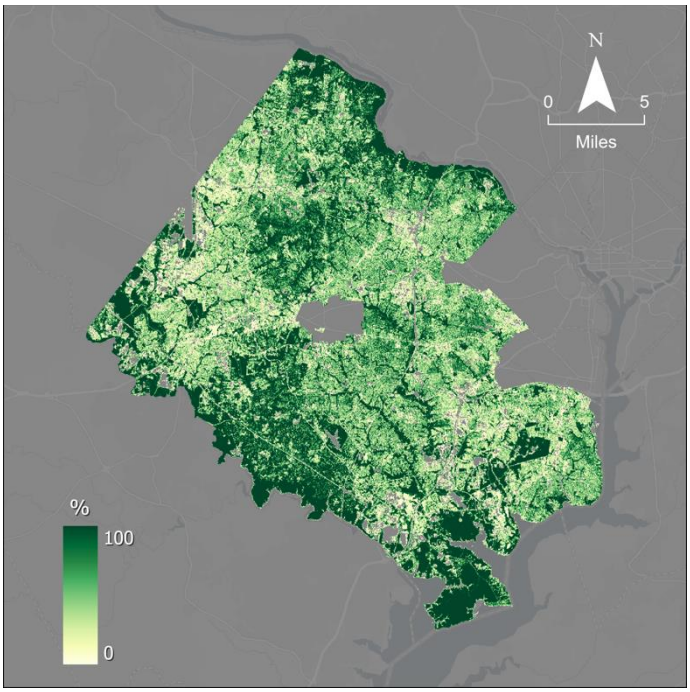

Figure B1. Percent Tree Canopy Cover

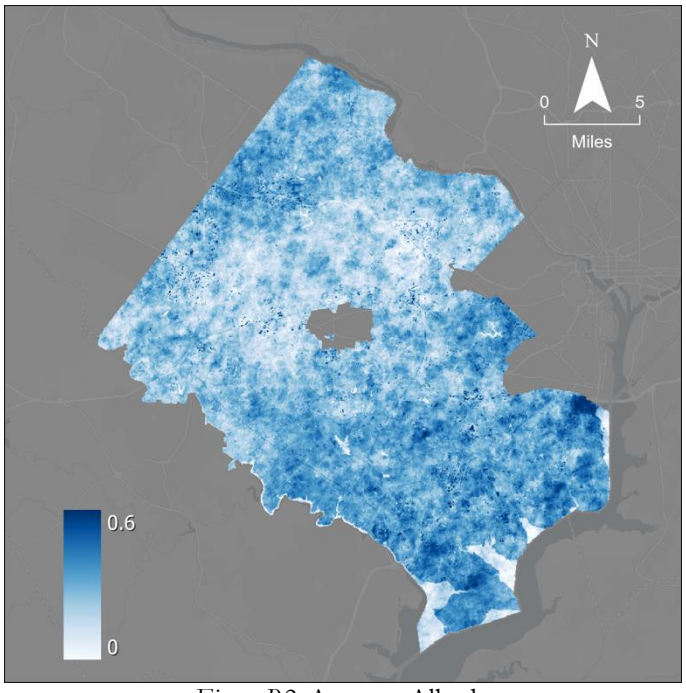

Figure B2. Average Albedo

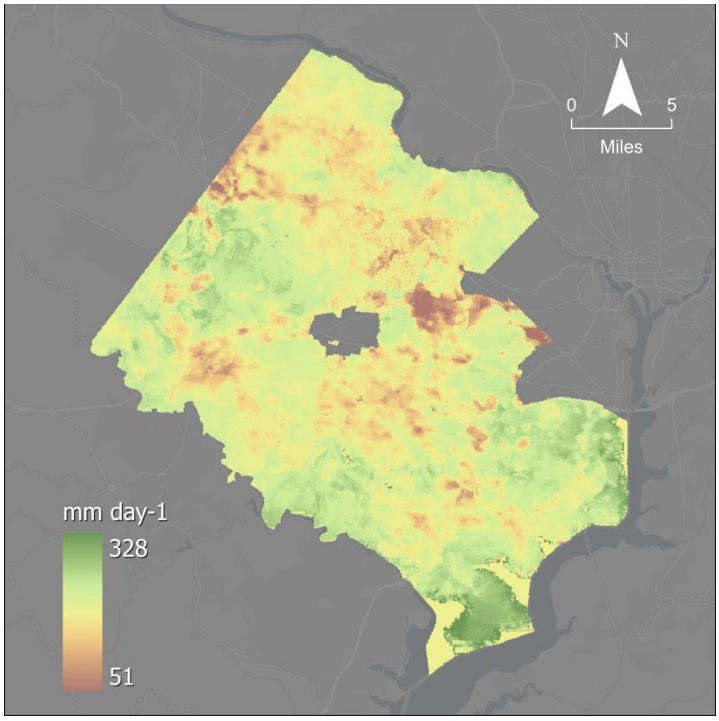

Figure B3. Evapotranspiration

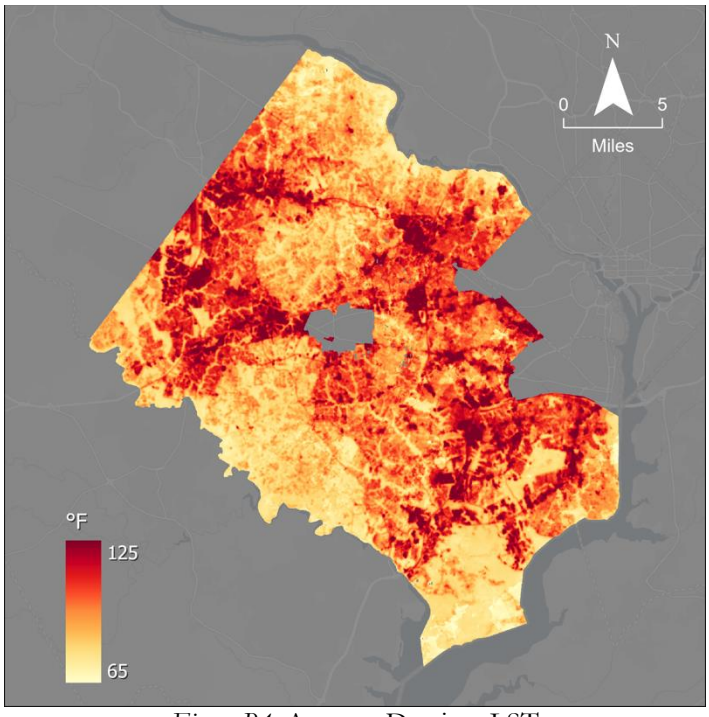

Figure B4. Average Daytime LST